bioRxiv preprint doi: https://doi.org/10.1101/2020.07.07.192153; this version posted July 7, 2020. The copyright holder for this preprint (which was not certified by peer review) is the author/funder. All rights reserved. No reuse allowed without permission.

1 **New insights into TNFα/PTP1B and PPARγ pathway through RNF213- a link between**
2 **inflammation, obesity, insulin resistance and Moyamoya disease**

3 Priyanka Sarkar and Kavitha Thirumurugan*

4 206, Structural Biology Lab, Centre for Biomedical Research, School of Biosciences &
5 Technology, Vellore Institute of Technology, Vellore-632014, India

6 * m.kavitha@vit.ac.in

7

8 **Acknowledgements**

9 This work has been financially supported by Vellore Institute of Technology's Seed grant and
10 Senior Research Fellowship by ICMR (Indian Council of Medical Research).

11 **Conflict of interest**

12 The authors declare that they have no conflict of interest.

13

14

15

bioRxiv preprint doi: https://doi.org/10.1101/2020.07.07.192153; this version posted July 7, 2020. The copyright holder for this preprint (which was not certified by peer review) is the author/funder. All rights reserved. No reuse allowed without permission.

16 **Abstract**

17 Diabetic patients are always at a higher risk of ischemic diseases like coronary artery
18 diseases. One such ischemic carotid artery disease is Moyamoya. Moyamoya disease (MMD)
19 has been associated with diabetes Type-I and II and the causality was unclear. RNF213 is the
20 major susceptible gene for MMD. To understand the association between diabetes mellitus
21 and MMD we chose the major players from both the anomalies, insulin and RNF213. But
22 before establishing a role of RNF213 in insulin regulating pathway we had to understand the
23 involvement of RNF213 within different biological systems. For this we have adopted a
24 preliminary computational approach to understand the prominent interactions of RNF213.
25 Our first objective was to construct an interactome for RNF213. We have analyzed several
26 curated databases and adapted a list of RNF213 interacting partners to develop its
27 interactome. Then to understand the involvement of this interactome in biological functions
28 we have analyzed major biological pathways, biological processes and prominent clusters
29 related to this interactome through computational approach. Then to develop a pathway that
30 might give clue for RNF213 involvement in insulin regulatory pathway we have validated the
31 intercluster and intracluster predictions and identified a regulatory pathway for RNF213.
32 RNF213 interactome was observed to be involved in adaptive immunity with 4 major
33 clusters; one of the cluster involved TNFα. Immune system involves several pathways, and
34 therefore at this point we have chosen an event-based strategy to obtain an explicit target.
35 Immunity is mediated by many pro-inflammatory cytokines like TNFα. TNFα-mediated
36 inflammation, obesity and insulin resistance are associated. Therefore we chose to explore the
37 role of RNF213 in TNFα-mediated inflammation in macrophages and inflammation-mediated
38 insulin-resistance in adipocytes. We have observed an enhancement of RNF213 gene
39 expression by LPS mediated pro-inflammatory stimuli and suppression by PPARγ-mediated
40 anti-inflammatory, insulin sensitizing stimuli in macrophages. A more significant response

bioRxiv preprint doi: https://doi.org/10.1101/2020.07.07.192153; this version posted July 7, 2020. The copyright holder for this preprint (which was not certified by peer review) is the author/funder. All rights reserved. No reuse allowed without permission.

41 was observed in adipocytes as well. Administration of the pro-inflammatory cytokine TNFα
42 was able to impede the reduction in RNF213 expression during adipogenesis and this effect
43 was observed to be mediated by PTP1B. Inactivation of PTP1B abolished RNF213
44 expression which in turn enhanced the adipogenesis process through enhanced PPARγ.
45 Constitutive expression of RNF213 suppressed the adipocyte differentiation by the inhibition
46 of PPARγ. We could show the expression of RNF213 has been regulated by TNFα/PTP1B
47 pathway and PPARγ. The constitutive expression of RNF213 during adipogenesis appears to
48 be an adipostatic measure that obese patients acquire to inhibit further adipogenesis. This is
49 verified *in silico* by analyzing the gene expression data obtained from Gene Expression
50 Omnibus database, which showed a higher expression of RNF213 in adipose tissue samples
51 of obese people. Overall this study gives new insights in the TNFα-mediated pathway in
52 adipogenesis and suggests a role of RNF213 in adipogenesis via this pathway.

53 **Keywords:** RNF213, *in silico* interactome analysis, TNFα, inflammation, insulin-resistance,
54 PTP1B, PPARγ, adipogenesis

55

56 **Introduction**

57 Diabetic patients have been marked at a higher risk of coronary artery diseases lead by
58 ischemic injury (Howangyin & Silvestre, 2014). This has made Diabetes mellitus a leading
59 cause for stroke and microvasculature impairments in brain (Ergul, Kelly-Cobbs, Abdalla, &
60 Fagan, 2012). Diabetes has been enormously linked to cerebrovascular diseases (Dalal &
61 Parab, 2002; Zhou, Zhang, & Lu, 2014). Moyamoya disease is an ischemic cerebrovascular
62 disease of carotid arteries. RNF213 (Ring Finger Protein 213) the founder susceptible gene
63 for MMD has been extensively studied to elucidate its role in the pathogenesis of Moyamoya
64 disease (Fujimura et al., 2014; Kamada et al., 2011; Kim, 2016; Shoemaker et al., 2015).
65 MMD is characterized by sprouting of vessels at the base of the brain and stenosis of internal

bioRxiv preprint doi: https://doi.org/10.1101/2020.07.07.192153; this version posted July 7, 2020. The copyright holder for this preprint (which was not certified by peer review) is the author/funder. All rights reserved. No reuse allowed without permission.

66 carotid artery caused by hyperplasia of smooth muscle cells present in the intima of carotid
67 arteries. This is sometimes accompanied by lipid accumulation in the proliferating intima
68 which ultimately leads to occlusion due to reduction in the lumen space of carotid arteries (J.
69 Suzuki & Takaku, 1969; Yamauchi et al., 2000). This is quite similar to the condition
70 observed in Type 2 diabetes complications leading to stroke (Zhou et al., 2014). Further
71 MMD has been associated to type 2 Diabetes mellitus in some reports, through their clinical
72 investigations (S. Suzuki et al., 2011). Study by Hatasu Kobayashi, suggested the
73 involvement of RNF213 in type I Diabetes mellitus. They showed that ablation of RNF213
74 retarded the progression of diabetes in Akita mice (H. Kobayashi et al., 2013). Akita mice are
75 model for type I Diabetes mellitus with a mutation in Ins2 (Pre-proinsulin 2).

76 RNF213 is an E3 ubiquitin ligase with AAA^+ ATPase domain and a RING domain to perform
77 the ligase activity (Morito et al., 2014). Though most of the previous studies had focused on
78 its physiological and clinical aspects, few independent studies suggested potential regulatory
79 mechanism for RNF213. Study by Scholz suggested RSPO3 (R-spondin3) as a co-regulatory
80 gene for RNF213 (Scholz et al., 2016). Another study by Kazuhiro Ohkubo suggested that
81 RNF213 is transcriptionally activated by the synergistic effect of TNFα and IFNγ in
82 endothelial cells, and PKR and PI3K-AKT pathways act as upstream regulators for these
83 cytokines. Also they revealed the involvement of RNF213 in inflammation through detailed
84 analysis of curated datasets (Ohkubo et al., 2015). It is still not known whether these
85 cytokines directly regulate the transcription of RNF213 or indirectly through some
86 downstream regulators. Further, RNF213 protein was reported to be a substrate for PTP1B
87 (Banh et al., 2016). PTP1B is a negative regulator of insulin (Nieto-Vazquez et al., 2007).
88 TNFα is also known to cause insulin resistance (Lorenzo et al., 2008). It also acts as an anti-
89 adipogenic factor in a way through altering PTP1B (D. D. Song et al., 2013). Also, these
90 cytokine-mediated pro-inflammatory molecules are secreted by activated macrophages.

bioRxiv preprint doi: https://doi.org/10.1101/2020.07.07.192153; this version posted July 7, 2020. The copyright holder for this preprint (which was not certified by peer review) is the author/funder. All rights reserved. No reuse allowed without permission.

91 When a host is invaded by a pathogen, dendritic cells are the first to get triggered, followed
92 by macrophages. Activated macrophages and dendritic cells act as effector phase molecule
93 for the adaptive immunity by engulfing, processing and presenting the antigens on its surface
94 to T_H cells and activates inflammation (Cronkite & Strutt, 2018; Janeway, P, M, & Al., 2001;
95 N. F. and K. Kobayashi, 2005). Inflammation has been extensively studied in relation to
96 obesity. Though obesity is stated as a low grade inflammation, pro-inflammatory cytokines
97 are known to act as negative regulators for adipocyte differentiation.

98 All these studies gave valuable insights about the regulatory mechanism that might cue the
99 involvement of RNF213. But a detailed analysis of the plausible interactome for RNF213 has
100 not been performed.

101 Therefore, we have adopted an *in silico* approach to predict an interactome for RNF213.
102 Gene co-regulatory and gene ontology studies have always been valued for predicting the
103 functional attributes of a gene. Several tools are available online to predict accurate hits
104 which can further be screened and validated and we applied this methodology as a base for
105 our study. Based on these findings we have designed the study to validate some of our *in*
106 *silico* predictions and explored new insights into an already existing anti-adipogenic insulin
107 regulatory pathway.

108

109 Results and Discussion

110 *In silico* analysis

111 The predicted interactome of RNF213 (Figure 1) was observed to be involved in several
112 biological systems (Figure2a) but mainly involved in immunity and cytokine driven
113 bioprocesses (Figure 2b) among which MHC Class1 antigen processing and presentation in
114 immune system was the major hit (Figure 2c). There were four major gene clusters (Figure

bioRxiv preprint doi: https://doi.org/10.1101/2020.07.07.192153; this version posted July 7, 2020. The copyright holder for this preprint (which was not certified by peer review) is the author/funder. All rights reserved. No reuse allowed without permission.

115 3a) observed to be functioning within the interactome. One of the clusters belongs to RNF213
116 and it had 12 members including RNF213. Among the observed list of proteins, DTX3L,
117 TRIM21 and HERC6 were co-regulated with RNF213 (Supplementary data 3). Each cluster
118 belongs to members having similar function within a biological system. Among these 4
119 clusters, other 2 clusters belong to members involved in inflammation and host defense
120 immune responses. One cluster included NOTCH1 (Fazio & Ricciardiello, 2016; Toshihiro
121 Ito, Judith M. Connett, Steven L. Kunkel, 2012) and the other cluster belong to TNFα and
122 PTP1B (G. J. Song et al., 2016; Zabolotny et al., 2008). The fourth cluster represented the
123 ATP synthase members. Macrophages were selected as *in vitro* model to validate the *in*
124 *silico* predictions. Macrophages are the key effectors and modulator cells of immune system
125 (Martinez & Gordon, 2014). Raw 264.7 murine macrophages were chosen because they are
126 activated on encountering pathogens similar to dendritic cells. Macrophages engulf these
127 pathogens and digest the antigen into smaller peptides which are presented to $CD8^+$ T cells
128 on MHC class I molecules (Cronkite & Strutt, 2018). Macrophages are also known to secrete
129 inflammatory molecules and trigger inflammation directly (Janeway et al., 2001; N. F. and K.
130 Kobayashi, 2005). Therefore, macrophages were chosen as an efficient model for intercluster
131 and intracluster validation.

132
133
134 **Intercluster and intracluster validation**

135 Raw 264.7 cells were stimulated with LPS. LPS induces classical activation of macrophages
136 (Martinez & Gordon, 2014) by enhancing the secretion of pro-inflammatory cytokine, TNFα
137 (Reis et al., 2012; Soromou et al., 2012). When these cells were treated with LPS, it induced
138 the expression of RNF213 at transcriptional level. Expression of TNFα and RNF213 was
139 pronounced after six hours of activation with LPS (Figure3**b**). Along with this, the co-
140 regulated members of RNF213 cluster were also analyzed to check whether they too show

bioRxiv preprint doi: https://doi.org/10.1101/2020.07.07.192153; this version posted July 7, 2020. The copyright holder for this preprint (which was not certified by peer review) is the author/funder. All rights reserved. No reuse allowed without permission.

141 similar expression profile on LPS stimulation. Interestingly, HECT and RLD domain
142 containing E3 ubiquitin protein ligase family member 6(HERC6), Tripartite motif-containing
143 protein 21 (TRIM21), Deltex E3 Ubiquitin Ligase 3L (DTX3L) displayed a similar
144 expression profile (Figure3**c**) to that of RNF213 and TNFα (Fig.3**b**). Thus members of
145 RNF213 cluster were properly grouped as they were regulated in a similar fashion by the
146 inflammatory stimulus, thereby validating the intra-cluster grouping. In contrast to the co-
147 regulated genes, F-box/LRR-repeat protein 7 (FBXL7) though being a member of the same
148 cluster had some variations with respect to the pattern of RNF213 expression pattern (Figure
149 3**b**). Similarity between TNFα expression pattern from the other cluster and the expression
150 pattern of members of RNF213 cluster, indicates an intercluster interaction. At this stage we
151 have concluded that TNFα individually might also be able to regulate RNF213.

152 TNFα is stated as an interlinking node between insulin resistance, obesity and inflammation.
153 It mediates Wnt and inflammation signaling to prevent adipocyte differentiation (Gustafson
154 & Smith, 2006) in 3T3-L1 by suppressing adipogenic genes (Ruan, Hacohen, Golub, Parijs,
155 & Lodish, 2002) and also by impeding the reduction of PTP1B (D.D. Song et al., 2013).

156 **RNF213 Expression in Adipocytes**

157 Therefore to link inflammation and adipogenesis we have attempted to evaluate the
158 expression of RNF213 in adipocytes. We observed RNF213 was expressed well during the
159 first 2 days of adipocyte differentiation and on the 8th day (Figure 4a). There was an inclined
160 suppression of RNF213 expression from 4th day onwards up to 6th day. This is the time when
161 the preadipocyte differentiate into mature adipocytes. In parallel to the regulation of RNF213
162 we also profiled PTP1B expression that was observed to be similar to that of RNF213
163 expression during adipocyte differentiation (Figure 4b). This suggested an involvement of
164 major adipogenic regulators like PPARγ and CEBPα in RNF213 regulation. Therefore, we

bioRxiv preprint doi: https://doi.org/10.1101/2020.07.07.192153; this version posted July 7, 2020. The copyright holder for this preprint (which was not certified by peer review) is the author/funder. All rights reserved. No reuse allowed without permission.

165 have evaluated the effect of relation between RNF213, PPARγ and CEBPα expression
166 pattern. CEBPα was not considered for further analysis because it was not synchronized with
167 the expression profile of RNF213 (data not shown). Therefore, we have evaluated the effect
168 of PPARγ on RNF213.

169 **Suppression of RNF213 by PPARγ agonist**

170 PPARγ is a master regulator of adipogenesis and it is activated by thiazolidinediones. Here
171 we have administered pioglitazone. Pioglitazone is not only an activator of PPARγ but it also
172 acts as an anti-inflammatory molecule by suppressing TNFα expression both at protein and
173 mRNA level by activating PPARγ and inactivating NFκB (Ao et al., 2010). It also suppresses
174 the expression of IFNγ in a PPARγ dependent manner(Cunard et al., 2019). Further it
175 decreases the insulin resistance (Kemnitz et al., 1994). Therefore, we have evaluated the
176 effect of pioglitazone treatment in macrophages as well as in adipocytes.

177 RNF213 was induced by inflammation and slightly suppressed by PPARγ dependent anti-
178 inflammation in macrophages (Figure 5a). Pioglitazone acted as an anti-inflammatory
179 molecule by completely suppressing the expression of TNFα (Figure 5a). Further, there was a
180 significant reduction in the mRNA expression of RNF213 in pioglitazone treated 3T3-L1
181 adipocytes (Figure 5b). These results indicate insulin sensitivity and anti-inflammation might
182 negatively regulate RNF213 gene expression. We did not use PPARγ inhibitor or PPARγ -
183 RNAi at this stage because we wanted to evaluate the RNF213 expression pattern throughout
184 the adipogenesis process. But inhibiting PPARγ will block adipogenesis.

185 **Effect of TNFα on RNF213 expression**

186 We have attempted to evaluate the effect of pro-inflammatory, negative regulator of insulin,
187 TNFα on RNF213 expression. For this , 3T3-L1 pre-adipocytes were treated with TNFα at an

bioRxiv preprint doi: https://doi.org/10.1101/2020.07.07.192153; this version posted July 7, 2020. The copyright holder for this preprint (which was not certified by peer review) is the author/funder. All rights reserved. No reuse allowed without permission.

188 inflammatory dose causing adipostatic effect (Gustafson & Smith, 2006). The treatment of
189 TNFα impeded the reduction of RNF213 mRNA throughout adipogenesis (Figure 6a). We
190 again performed a parallel expression profiling for PTP1B. We observed a similar pattern in
191 PTP1B expression to that of RNF213 expression (Figure 6b). The same trend was seen in the
192 protein expression of RNF213 and PTP1B following TNFα treatment (Figure 7a-e).
193 Immunostained adipocyte cells were observed for RNF213 and PTP1B expression at day 2
194 and day 5 of differentiation. The cells treated with TNFα expressed RNF213 and PTP1B
195 throughout adipogenesis process (Figure 7a-d).

196 **Effect of PTP1B on RNF213 expression**

197 Further we wanted to investigate the mechanism followed by TNFα. Since PTP1B was
198 reported as one of the downstream partners of TNFα insulin resistance pathway and in our
199 data also it showed similar trend of expression to that of RNF213 expression. We have
200 evaluated the effect of PTP1B on RNF213. For this we have analysed the effect of PTP1B
201 inactivation on RNF213 expression. The administration of sodium orthovanadate
202 (phosphatase inhibitor) at 35 µM suppressed the mRNA expression of RNF213 (Figure8a).
203 Whereas using PTP1B inhibitor TCS401 specifically at 0.29 µM concentration abolished the
204 expression of RNF213 at gene level (Figure 8b) and protein level. This was indicated by *in*
205 *vitro* protein expression analysis measured with fluorescently labelled antibodies (Figure7f).
206 Further when TNFα treated cells were co-treated with TCS401, it nullified the TNFα
207 mediated enhanced effect on RNF213 expression (Figure 7e). Day 8 adipocytes treated with
208 TNFα show reduced adipogenesis indicated by less number of Oil Red O stained lipid
209 droplets (Figure 9a-ii) and PPARγ transcript levels (Figure 9b) . Same cells with TCS401 co-
210 treatment show enhanced number of lipid droplets suggesting the role of PTP1B on
211 adipogenesis (Figure 9a-iii).

bioRxiv preprint doi: https://doi.org/10.1101/2020.07.07.192153; this version posted July 7, 2020. The copyright holder for this preprint (which was not certified by peer review) is the author/funder. All rights reserved. No reuse allowed without permission.

212 This indicated that TNFα can also regulate RNF213 and it is mediated through PTP1B. This
213 data showed a complete regulatory dependence of RNF213 on PTP1B.

214 **Effect of positive regulators of RNF213 (TNFα and PTP1B) on PPARγ**

215 Since RNF213 expression was observed to be suppressed by activation we wanted to analyze
216 the effects of positive regulators of RNF213 on PPARγ, the negative regulator of RNF213.

217 First we have evaluated the gene expression pattern of PPARγ in normal differentiating cells
218 and then compared it with the TNFα treated differentiating cells and PTP1B inhibited
219 differentiating cells. Gene expression of PPARγ was high in adipocytes treated with DIM
220 (differentiation induction media) particularly at day 8 (Figure 9b). PPARγ expression was
221 very low in the cells treated with TNFα. This effect was reversed in cells treated with PTP1B
222 specific inhibitor TCS401 (Figure 9b), the downstream partner of TNFα. This shows that
223 administration of TNFα suppresses PPARγ in the presence of PTP1B. TNFα affects several
224 adipogenic molecules through different pathways. Therefore PPARγ could be acting
225 downstream to PTP1B or it might have its own regulatory pathway to modulate RNF213
226 expression.

227 The inactivation of PTP1B individually also increased adipogonesis as indicated by the
228 increased number of lipid droplets (Figure 10) and PPARγ expression levels (Figure 9b).
229 Therefore PTP1B might be regulating RNF213 through PPARγ and further analysis is
230 required to evaluate this mechanism.

231 **Gene expression analysis from Microarray database**

232 Our data suggest the involvement of RNF213 in adipocyte differentiation. This is in
233 accordance to the gene expression data curated from Gene Expression Omnibus through
234 GEO2R tool, where we can observe a 4.5 fold increase in RNF213 expression in non-diabetic

bioRxiv preprint doi: https://doi.org/10.1101/2020.07.07.192153; this version posted July 7, 2020. The copyright holder for this preprint (which was not certified by peer review) is the author/funder. All rights reserved. No reuse allowed without permission.

235 obese PIMA individuals (Supplementary data 4). This was the only curated normalized
236 dataset available that significantly recognized RNF213.

237 Most of the other datasets had variable probes for RNF213 with unreliable Padj values.
238 Therefore we chose this dataset for our evaluation. Obesity is said to be a low grade/chronic
239 inflammation which leads to insulin resistance (Choi & Cohen, 2017). An increase in the
240 gene expression of RNF213 during obesity suggests its role in obesity related insulin
241 resistance and predicts its likely protective effect in obese patients by reducing adipogenesis.

242 **Perspectives and Conclusion**

243 It is decisive to mark the interacting partners for the gene to know the exact role and the
244 regulatory mechanism of a gene. RNF213 is observed to be present across many uncurated
245 datasets, making it relevant to list the plausible interactors. By curating such datasets we have
246 observed that RNF213 shows an increased gene expression during obese conditions.
247 RNF213 has been reported to be induced by inflammatory stimuli (Ohkubo et al., 2015) and
248 its ablation improves glucose tolerance (H. Kobayashi et al., 2013). These reports are in
249 accordance with our study showing the induction of RNF213 expression by TNFα/PTP1B
250 inflammatory pathway leading towards adipostatic effects. This pathway is known to be
251 involved in insulin resistance in adipocytes (Lorenzo et al., 2008). Our data also shows the
252 continuous expression of RNF213 downstream to PTP1B suppresses adipogenesis. But its
253 ablation by PTP1B inactivation increases adipogenesis. Further there is a cyclic pattern of
254 RNF213 expression suggesting the existence of a feedback inhibition mechanism to regulate
255 RNF213. In this study, we had predicted a whole curated interactome for RNF213 which is
256 partly validated. This prediction highlighted the emerging role of RNF213 in inflammation
257 and inflammation mediated anti-adipogenesis. Also we had speculated that TNFα/PTP1B
258 pathway positively regulates RNF213 expression and negatively regulates adipogenesis.

bioRxiv preprint doi: https://doi.org/10.1101/2020.07.07.192153; this version posted July 7, 2020. The copyright holder for this preprint (which was not certified by peer review) is the author/funder. All rights reserved. No reuse allowed without permission.

259 Further RNF213 knockdown analysis is required to confirm the influential role of RNF213 in
260 TNFα/PTP1B mediated insulin resistance and adipostasis.

261 From our data it was clear that a reduction in RNF213 expression was required to achieve
262 adipogenesis and this reduction was caused by the activation of PPARγ; indicating PPARγ as
263 an effective regulator of RNF213. RNF213 is expressed in both macrophages as well as
264 adipocytes. Both these cell types are related to inflammation. TNFα looks like the common
265 regulator of RNF213 via PTP1B but PPARγ appears to be more effective in suppressing
266 RNF213 in adipocytes suggesting a link between adipogenesis, insulin resistance,
267 inflammation and MMD via TNFα, PTP1B, PPARγ and RNF213. PTP1B might be
268 inactivating PPARγ in order to induce RNF213, and TNFα and PTP1B is known to suppress
269 PPARγ. Further analysis is required to state whether PPARγ modulates RNF213 through this
270 pathway or some other pathway. Overall TNFα/PTP1B insulin-resistant pathway enhances
271 RNF213 expression whereas PPARγ mediated insulin sensitization suppresses its expression.
272 Therefore RNF213 could be another link between obesity, inflammation, insulin resistance
273 and MMD like TNFα.

274

275 **Methods**

276 **Interactome prediction**

277 A molecular interactome was predicted using protein interactors and gene interactors.
278 Interacting genes were listed down from UCSC Genome Browser's gene interaction tool and
279 GeneMania. Protein-protein interactions were based on literature survey, physical interactors,
280 co-expressed partners and functional homology transfers. Physical interactors and co-
281 expressed partners were sorted through GeneMania and STRING. The functional homologs
282 were detected through Genedecks online web tool. These homologous functional partners
283 were sorted based on domain matching and the protein interactors for these partners were

bioRxiv preprint doi: https://doi.org/10.1101/2020.07.07.192153; this version posted July 7, 2020. The copyright holder for this preprint (which was not certified by peer review) is the author/funder. All rights reserved. No reuse allowed without permission.

284 listed as homology transfer interactions. All the interactions were sorted based on their
285 probability matching and false discovery rate (FDR). The value 0.01 was considered as a
286 cutoff for FDR. List of these molecules (Supplementary data 1) were used to predict a
287 molecular interactome dataset and it was uploaded on STRING database to develop a visual
288 interacting network with high confidence (0.7). A diagrammatic representation of this
289 approach has been given in the attachments as flow chart for interactome prediction.
290
291 **Interactome validation and pathway prediction**
292 The obtained interactome dataset was submitted to METASCAPE to obtain enrichment
293 cluster analysis and functional complexes through EXPRESS Analysis. METASCAPE results
294 were verified through DAVID. Members of the interactome dataset were submitted to
295 REACTOME to confirm the biological systems and pathway analysis. These results were
296 confirmed through KEGG PATHWAY by considering the KEGG ontology terms for these
297 molecules. The major complexes as presented by the use of MCODE algorithm were based
298 on the top non-redundant enriched terms from METASCAPE and the biological system
299 pathway from REACTOME. The members of these complexes were analyzed for their co-
300 regulation through Database of Gene Co-Regulation (dGCR) (Williams, 2015) and validated
301 for their co-regulated expression and ligand stimulated regulatory pathway in cell lines.
302
303 **Cell culture**
304 RAW 264.7 cells and 3T3-L1 cells were bought from NCCS (Pune) cell repository, India.
305 RAW 264.7 cells were cultured in DMEM (Himedia) and 10% FBS (Invitrogen, USA) media
306 containing 1% antibiotic-antimycotic solution (100X, Gibco) as described previously
307 (George, Ramasamy, & Sirajudeen, 2019). The 3T3-L1 pre-adipocytes were grown as
308 previously described (Shihabudeen, Roy, James, & Thirumurugan, 2015). Briefly, cells were

bioRxiv preprint doi: https://doi.org/10.1101/2020.07.07.192153; this version posted July 7, 2020. The copyright holder for this preprint (which was not certified by peer review) is the author/funder. All rights reserved. No reuse allowed without permission.

309 grown for 2 days post confluence in DMEM (Invitrogen, USA) supplemented with 10% new
310 born calf serum (Invitrogen, USA). Differentiation was then induced by changing the
311 medium to DMEM supplemented with 10% fetal bovine serum, 0.5 mM 3-isobutyl-1-
312 methylxanthine, 1 μM dexamethasone, and 1.2 μM insulin (Sigma-Aldrich, USA). After 48
313 h, the differentiation medium (referred to as DIM) was replaced with maintenance medium
314 containing DMEM supplemented with 10% fetal bovine serum and 1.2 μM insulin for 48
315 hours post induction. Thereafter maintenance medium was replaced every 48 h until 14 days.
316 Cells were incubated at 37°C in a 5% CO_2 environment.
317
318 **Treatment and sample collection**
319 Raw 264.7 cells were treated with 1μg/ml of LPS to induce inflammation. These cells were
320 collected at different time points; post induction (1h, 3h, 6h, 12h and 24h) and gene
321 expression for the samples were normalized against samples from un-induced Raw 264.7
322 cells. PPARγ activation for these cells was done by treating the cells with 10μM
323 concentration of pioglitazone.
324
325 Samples for 3T3-L1 cells were collected at different time points after inducing with
326 differentiation media (at hours (h) 0h, 2h, 4h, 7h, 9h, 12h, 24h, 48h, and at days 4, 6, 8, 10,
327 12, 14). Sodium orthovanadate (Sigma) was administered at a concentration of 35 μM as
328 reported previously along with DIM (Liao & Lane, 1995). TNFα (Sigma) was administered at
329 a concentration of 1.5 ng/ml along with DIM and maintenance media up to 12 days. This
330 concentration was chosen based on the previous reports of TNFα causing inflammatory
331 response in 3T3-L1 cells (Gustafson & Smith, 2006).TCS401, specific inhibitor of PTP1B
332 (Veda scientific) (Iversen et al., 2000) was administered at a concentration of 0.29 μM along
333 with DIM and maintenance media up to 8 days. Gene expression for the samples collected at

bioRxiv preprint doi: https://doi.org/10.1101/2020.07.07.192153; this version posted July 7, 2020. The copyright holder for this preprint (which was not certified by peer review) is the author/funder. All rights reserved. No reuse allowed without permission.

334 different time points were normalized against samples from 48 hours pre-induction (referred
335 to as -2 day or control) for 3T3-L1 cells.
336

337 **Gene expression**

338 Total RNA was isolated using TRIzol reagent according to manufacturer's instructions
339 (Invitrogen, USA). The cDNA was synthesized from 1 μg of total RNA using the Prime
340 script cDNA conversion kit (Takara, India). Gene expression was measured using SYBR
341 green dye (Takara, India) in BIORAD CFX96 Touch Real-Time PCR Detection System.
342 GAPDH was used as an endogenous control in the comparative cycle threshold (CT) method.
343 The list of primers from Xcelris is given in the Supplementary data 2.
344

345 **Oil Red O staining**

346 Oil Red O staining was performed following a modified protocol previously described (Kraus
347 et al., 2016). Briefly, cells were fixed with 10% formalin for 45 minutes followed by a
348 washing step with 60% isopropanol. Then the cells were air dried and incubated with Oil Red
349 O stain (Sigma) for 30 minutes. Then the cells were washed properly with distilled water and
350 the dried wells were used for imaging. Imaging was done through Olympus Magnus Phase
351 contrast microscope.
352

353 **Immunocytochemistry**

354 3T3-L1 adipocyte cells were fixed with 4% PFA (paraformaldehyde) for 15 minutes at room
355 temperature, washed with PBS and permeabilized with 0.3 % of TRITON X-100 for 10 min.
356 After blocking the cells with blocking buffer (0.3% TRITON X-100, 1% BSA) for 1 hour;
357 the cells were incubated for 5 hours at 4ºC with specific primary antibody (Alexa488 tagged
358 RNF213 primary antibody and Cy3 tagged PTP1B primary antibody from BIOSS, USA) and

bioRxiv preprint doi: https://doi.org/10.1101/2020.07.07.192153; this version posted July 7, 2020. The copyright holder for this preprint (which was not certified by peer review) is the author/funder. All rights reserved. No reuse allowed without permission.

359 then counterstained with DAPI. Samples were collected on day 1, day 2, day 5 and day 7.
360 Imaging was done by using EVOS FLoid imaging station (Thermo Fischer, USA) with 20x
361 fluorite objective and LED light cubes containing hard coated filters (blue, red and green).
362

363 **Gene expression analysis from Microarray database**

364 RNF213 differential expression was re-analyzed in human samples through GEO2R. GEO2R
365 is the R-package offered by Gene Expression Omnibus (GEO) to obtain differentially
366 expressed gene list in a given microarray dataset based on the Fold change and AdjP-values.
367 For this study we have used the dataset accession number GSE2508 from GEO database.
368 GSE2508 dataset comprises of RNA samples isolated from the adipocytes of abdominal
369 subcutaneous fat of non-diabetes Pima Indians (Y. H. Lee, S. Nair, E. Rousseau, P. A.
370 Tataranni, C. Bogardus, P. A. Permana, 2006).
371

372 **Statistical analysis**

373 Each experiment had a lower limit of n=3 (3 biological replicates with 3 technical replicates
374 taken as average).Some experiments were repeated more number of times to confirm
375 accuracy. All data were presented as mean ± SEM. Column statistics and ANOVA was
376 performed using Graphpad Prism v.06 software package. $P< 0.05$ was considered to be
377 statistically significant. It is presented as ns ($p> 0.05$), *($p \leq 0.05$), **($p \leq 0.01$), ***($p \leq$
378 0.001) **** ($p \leq 0.0001$).
379

380 **References**

381 Ao, C., Huo, Y., Qi, L., Xiong, Z., Xue, L., & Qi, Y. (2010). Pioglitazone suppresses the
382 lipopolysaccharide-induced production of inflammatory factors in mouse macrophages

bioRxiv preprint doi: https://doi.org/10.1101/2020.07.07.192153; this version posted July 7, 2020. The copyright holder for this preprint (which was not certified by peer review) is the author/funder. All rights reserved. No reuse allowed without permission.

383 by inactivating NF- k B, *34*, 723–730. https://doi.org/10.1042/CBI20090005

384 Banh, R. S., Iorio, C., Marcotte, R., Xu, Y., Cojocari, D., Zhang, S., … Habu, T. (2016).
385 PTP1B regulates non -mitochondrial oxygen consumption via RNF213 to promote
386 tumour survival during hypoxia, *18*(7), 803–813.
387 https://doi.org/10.1038/ncb3376.PTP1B

388 Choi, C. H. E. E. J., & Cohen, P. (2017). How does obesity lead to insulin resistance?
389 *Epigenetics*, 2–3. https://doi.org/10.7554/eLife.30766

390 Cronkite, D. A., & Strutt, T. M. (2018). The Regulation of Inflammation by Innate and
391 Adaptive Lymphocytes, *2018*.

392 Cunard, R., Eto, Y., Muljadi, J. T., Christopher, K., Kelly, C. J., & Ricote, M. (2019).
393 Repression of IFN- γ Expression by Peroxisome Proliferator-Activated Receptor γ, *172*,
394 7530–7536. https://doi.org/10.4049/jimmunol.172.12.7530

395 Dalal, P. M., & Parab, P. V. (2002). Cerebrovascular disease in type 2 diabetes mellitus.
396 *Neurology India*, *50*(4), 380–385.

397 Ergul, A., Kelly-Cobbs, A., Abdalla, M., & Fagan, S. C. (2012). Cerebrovascular
398 Complications of Diabetes: Focus on Stroke Adviye. *Endocr Metab Immune Disord*
399 *Drug Targets*, *12*(2), 148–158. https://doi.org/10.1038/jid.2014.371

400 Fazio, C., & Ricciardiello, L. (2016). Inflammation and Notch signaling : a crosstalk with
401 opposite effects on tumorigenesis. *Nature Publishing Group*, *7*(12), e2515-7.
402 https://doi.org/10.1038/cddis.2016.408

403 Fujimura, M., Sonobe, S., Nishijima, Y., Niizuma, K., Sakata, H., Kure, S., & Tominaga, T.
404 (2014). Genetics and Biomarkers of Moyamoya Disease: Significance of RNF213 as a

bioRxiv preprint doi: https://doi.org/10.1101/2020.07.07.192153; this version posted July 7, 2020. The copyright holder for this preprint (which was not certified by peer review) is the author/funder. All rights reserved. No reuse allowed without permission.

405 Susceptibility Gene. *Journal of Stroke*, *16*(2), 65–72.
406 https://doi.org/10.5853/jos.2014.16.2.65

407 George, L., Ramasamy, T., & Sirajudeen, K. N. S. (2019). LPS-induced Apoptosis is
408 Partially Mediated by Hydrogen Sulphide in RAW 264 . 7 Murine Macrophages LPS-
409 induced Apoptosis is Partially Mediated by Hydrogen. *Immunological Investigations*, 1–
410 15. https://doi.org/10.1080/08820139.2019.1566355

411 Gustafson, B., & Smith, U. (2006). CYTOKINES PROMOTE WNT SIGNALING AND
412 INFLAMMATION AND IMPAIR THE NORMAL DIFFERENTIATION AND LIPID
413 ACCUMULATION IN Birgit Gustafson and Ulf Smith From the Lundberg Laboratory
414 for Diabetes Research , Department of Internal Medicine , The Sahlgrenska Academy.
415 *JBC Papers*. https://doi.org/10.1074/jbc.M512077200

416 Howangyin, K. Y., & Silvestre, J. S. (2014). Diabetes mellitus and ischemic diseases:
417 Molecular mechanisms of vascular repair dysfunction. *Arteriosclerosis, Thrombosis,*
418 *and Vascular Biology*, *34*(6), 1126–1135.
419 https://doi.org/10.1161/ATVBAHA.114.303090

420 Iversen, L. F., Andersen, S., Branner, S., Mortensen, S. B., Peters, H., Norris, K., … Møller,
421 H. (2000). Structure-based Design of a Low Molecular Weight , Nonphosphorus ,
422 Nonpeptide , and Highly Selective Inhibitor of Protein-tyrosine Phosphatase 1B. *The*
423 *Journal of Biological Chemistry*, *275*(14), 10300–10307.

424 Janeway, C. J., P, T., M, W., & Al., E. (2001). Principles of innate and adaptive immunity.
425 New York: Immunobiology.

426 Kamada, F., Aoki, Y., Narisawa, A., Abe, Y., Komatsuzaki, S., Kikuchi, A., … Kure, S.
427 (2011). A genome-wide association study identifies RNF213 as the first Moyamoya

bioRxiv preprint doi: https://doi.org/10.1101/2020.07.07.192153; this version posted July 7, 2020. The copyright holder for this preprint (which was not certified by peer review) is the author/funder. All rights reserved. No reuse allowed without permission.

428 disease gene. *Journal of Human Genetics*, *56*(1), 34–40.
429 https://doi.org/10.1038/jhg.2010.132

430 Kemnitz, J. W., Elson, D. F., Roecker, E. B., Baum, S. T., Bergman, R. N., & Meglasson, M.
431 D. (1994). Pioglitazone increases insulin sensitivity, reduces blood glucose, insulin, and
432 lipid levels, and lowers blood pressure, in obese, insulin-resistant rhesus monkeys.
433 *Diabetes*, *43*(2), 204–211. https://doi.org/10.2337/diab.43.2.204

434 Kim, J. S. (2016). Moyamoya Disease: Epidemiology, Clinical Features, and Diagnosis.
435 *Journal of Stroke*, *18*(1), 2–11. https://doi.org/10.5853/jos.2015.01627

436 Kobayashi, H., Yamazaki, S., Takashima, S., Liu, W., Okuda, H., Yan, J., … Koizumi, A.
437 (2013). Ablation of Rnf213 retards progression of diabetes in the Akita mouse.
438 *Biochemical and Biophysical Research Communications*, *432*(3), 519–525.
439 https://doi.org/10.1016/j.bbrc.2013.02.015

440 Kobayashi, N. F. and K. (2005). Macrophages in Inflammation. *Current Drug Targets -*
441 *Inflammation & Allergy*. https://doi.org/http://dx.doi.org/10.2174/1568010054022024

442 Kraus, N. A., Ehebauer, F., Zapp, B., Rudolphi, B., Kraus, B. J., & Kraus, D. (2016).
443 Quantitative assessment of adipocyte differentiation in cell culture. *Adipocyte*, *5*(4),
444 351–358. https://doi.org/10.1080/21623945.2016.1240137

445 Liao, K., & Lane, M. D. (1995). The blockade of preadipocyte differentiation by protein-
446 tyrosine phosphatase HA2 is reversed by vanadate. *The Journal of Biological Chemistry*,
447 *270*(20), 12123–12132. https://doi.org/10.1074/JBC.270.20.12123

448 Lorenzo, M., Fernández-Veledo, S., Vila-Bedmar, R., Garcia-Guerra, L., De Alvaro, C., &
449 Nieto-Vazquez, I. (2008). Insulin resistance induced by tumor necrosis factor-alpha in

bioRxiv preprint doi: https://doi.org/10.1101/2020.07.07.192153; this version posted July 7, 2020. The copyright holder for this preprint (which was not certified by peer review) is the author/funder. All rights reserved. No reuse allowed without permission.

450 myocytes and brown adipocytes. *Journal of Animal Science*, *86*(14 Suppl), E94-104.
451 https://doi.org/10.2527/jas.2007-0462

452 Martinez, F. O., & Gordon, S. (2014). The M1 and M2 paradigm of macrophage activation :
453 time for reassessment, *13*(March), 1–13. https://doi.org/10.12703/P6-13

454 Morito, D., Nishikawa, K., Hoseki, J., Kitamura, A., Kotani, Y., Kiso, K., … Nagata, K.
455 (2014). Moyamoya disease-associated protein mysterin/RNF213 is a novel AAA+
456 ATPase, which dynamically changes its oligomeric state. *Sci Rep*, *4*, 4442.
457 https://doi.org/10.1038/srep04442

458 Nieto-Vazquez, I., Fernández-Veledo, S., de Alvaro, C., Rondinone, C. M., Valverde, A. M.,
459 & Lorenzo, M. (2007). Protein-tyrosine phosphatase 1B-deficient myocytes show
460 increased insulin sensitivity and protection against tumor necrosis factor-alpha-induced
461 insulin resistance. *Diabetes*, *56*(2), 404–413. https://doi.org/10.2337/db06-0989

462 Ohkubo, K., Sakai, Y., Inoue, H., Akamine, S., Ishizaki, Y., Matsushita, Y., … Hara, T.
463 (2015). Moyamoya disease susceptibility gene RNF213 links inflammatory and
464 angiogenic signals in endothelial cells. *Scientific Reports*, *5*(August), 13191.
465 https://doi.org/10.1038/srep13191

466 Reis, J., Guan, X. Q., Kisselev, A. F., Papasian, C. J., Qureshi, A. A., Morrison, D. C., …
467 Qureshi, N. (2012). LPS-Induced Formation of Immunoproteasomes TNF-α and Nitric
468 Oxide Production are Regulated by Altered Composition of Proteasome-Active Sites,
469 *60*, 77–88. https://doi.org/10.1007/s12013-011-9182-8.LPS-Induced

470 Ruan, H., Hacohen, N., Golub, T. R., Parijs, L. Van, & Lodish, H. F. (2002). Tumor Necrosis
471 Factor-α Suppresses Adipocyte-Specific Genes and Activates Expression of
472 Preadipocyte Genes in 3T3-L1 Adipocytes. *Diabetes*, *51*, 1319–1336.

bioRxiv preprint doi: https://doi.org/10.1101/2020.07.07.192153; this version posted July 7, 2020. The copyright holder for this preprint (which was not certified by peer review) is the author/funder. All rights reserved. No reuse allowed without permission.

473 Scholz, B., Korn, C., Wojtarowicz, J., Mogler, C., Augustin, I., Boutros, M., … Augustin, H.
474 G. (2016). Endothelial RSPO3 Controls Vascular Stability and Pruning through Non-
475 canonical WNT/Ca2+/NFAT Signaling. *Developmental Cell*, *36*(1), 79–93.
476 https://doi.org/10.1016/j.devcel.2015.12.015

477 Shihabudeen, M. S., Roy, D., James, J., & Thirumurugan, K. (2015). Chenodeoxycholic acid,
478 an endogenous FXR ligand alters adipokines and reverses insulin resistance. *Molecular*
479 *and Cellular Endocrinology*, *414*, 19–28. https://doi.org/10.1016/J.MCE.2015.07.012

480 Shoemaker, L. D., Clark, M. J., Patwardhan, A., Chandratillake, G., Garcia, S., Chen, R., …
481 Steinberg, G. K. (2015). Disease Variant Landscape of a Large Multi-ethnic Population
482 of Moyamoya Patients by Exome Sequencing. *G3 (Bethesda)*, *6*(1), 41–49.
483 https://doi.org/10.1534/g3.115.020321

484 Song, D.-D., Chen, Y., Li, Z.-Y., Guan, Y.-F., Zou, D.-J., & Miao, C.-Y. (2013). Protein
485 tyrosine phosphatase 1B inhibits adipocyte differentiation and mediates TNFα action in
486 obesity. *Biochimica et Biophysica Acta (BBA) - Molecular and Cell Biology of Lipids*,
487 *1831*(8), 1368–1376. https://doi.org/https://doi.org/10.1016/j.bbalip.2013.05.006

488 Song, D. D., Chen, Y., Li, Z. Y., Guan, Y. F., Zou, D. J., & Miao, C. Y. (2013). Protein
489 tyrosine phosphatase 1B inhibits adipocyte differentiation and mediates TNFα action in
490 obesity. *Biochimica et Biophysica Acta - Molecular and Cell Biology of Lipids*, *1831*(8),
491 1368–1376. https://doi.org/10.1016/j.bbalip.2013.05.006

492 Song, G. J., Jung, M., Kim, J., Park, H., Rahman, H., Zhang, S., … Suk, K. (2016). A novel
493 role for protein tyrosine phosphatase 1B as a positive regulator of neuroinflammation.
494 *Journal of Neuroinflammation*, 1–14. https://doi.org/10.1186/s12974-016-0545-3

495 Soromou, L. W., Zhang, Z., Li, R., Chen, N., Guo, W., Huo, M., … Deng, X. (2012).

bioRxiv preprint doi: https://doi.org/10.1101/2020.07.07.192153; this version posted July 7, 2020. The copyright holder for this preprint (which was not certified by peer review) is the author/funder. All rights reserved. No reuse allowed without permission.

496 Regulation of Inflammatory Cytokines in Lipopolysaccharide-Stimulated RAW 264.7
497 Murine Macrophage by 7-O-Methyl-naringenin, 3574–3585.
498 https://doi.org/10.3390/molecules17033574

499 Suzuki, J., & Takaku, A. (1969). Cerebrovascular “moyamoya” disease. Disease showing
500 abnormal net-like vessels in base of brain. *Archives of Neurology*, *20*(3), 288–299.
501 https://doi.org/10.1001/archneur.1969.00480090076012

502 Suzuki, S., Mitsuyama, T., Horiba, A., Fukushima, S., Hashimoto, N., & Kawamata, T.
503 (2011). Moyamoya disease complicated by Graves’ disease and type 2 diabetes mellitus:
504 Report of two cases. *Clinical Neurology and Neurosurgery*, *113*(4), 325–329.
505 https://doi.org/10.1016/j.clineuro.2010.11.022

506 Toshihiro Ito, Judith M. Connett, Steven L. Kunkel, and A. M. (2012). Notch system in the
507 linkage of innate and adaptive immunity.

508 Williams, G. (2015). Database of Gene Co-Regulation (dGCR): A Web Tool for Analysing
509 Patterns of Gene Co-regulation across Publicly Available Expression Data. *Journal of*
510 *Genomics*, *3*. https://doi.org/10.7150/jgen.10888

511 Y. H. Lee, S. Nair, E. Rousseau, P. A. Tataranni, C. Bogardus, P. A. Permana, D. B. A. and
512 G. P. P. (2006). Microarray profiling of isolated abdominal subcutaneous adipocytes
513 from obese vs non-obese Pima Indians: increased expression of inflammation-related
514 genes. *Diabetologia*, *48*(9), 1776–1783.

515 Yamauchi, T., Tada, M., Houkin, K., Tanaka, T., Nakamura, Y., Kuroda, S., … Fukui, M.
516 (2000). Linkage of familial moyamoya disease (Spontaneous occlusion of the circle of
517 Willis) to chromosome 17q25. *Stroke*, *31*(4), 930–935.
518 https://doi.org/10.1161/01.STR.31.4.930

bioRxiv preprint doi: https://doi.org/10.1101/2020.07.07.192153; this version posted July 7, 2020. The copyright holder for this preprint (which was not certified by peer review) is the author/funder. All rights reserved. No reuse allowed without permission.

519 Zabolotny, J. M., Kim, Y., Welsh, L. A., Kershaw, E. E., Neel, B. G., & Kahn, B. B. (2008).
520 Protein-tyrosine Phosphatase 1B Expression Is Induced by Inflammation in Vivo,
521 *283*(21), 14230–14241. https://doi.org/10.1074/jbc.M800061200

522 Zhou, H., Zhang, X., & Lu, J. (2014). Progress on diabetic cerebrovascular diseases. *Bosnian*
523 *Journal of Basic Medical Sciences*, *14*(4), 185–190.
524 https://doi.org/10.17305/bjbms.2014.4.203

525

Figure Legends

Figure1 Predicted interactome of RNF213. The candidates of the interactome were grouped together in STRING database to visualize their interactions

Figure 2(a) Involvement of predicted interactome in several biological systems. (b) Enrichment process showing the predominance of interactome in immunity and inflammation. (c) Involvement of RNF213 in MHC class I antigen processing. Dynamic areas of RNF213 are encased in pink.

Figure 3 (a) There were four major gene clusters observed to be functioning within the interactome of RNF213. Each color represents a different biological function. **(**b) Treatment of Raw 264.7 cells with LPS induced the expression of TNFα and RNF213 and enhanced expression was noticed after six hours of activation (b) Expression profile of co-regulated members of RNF213 cluster (TRIM21, DTX3L, HERC6) and non-co-regulated member FBXL7 after LPS treatment.

Figure 4 (a)Expression of RNF213 at mRNA level during adipocyte differentiation. RNF213 expressed well during the first 2 days of adipocyte differentiation and on the 8th day. (b) Expression of PTP1Bat mRNA level during adipocyte differentiation. PTP1B expression pattern was similar to that of RNF213.

Figure 5 (a) Effect of pioglitazone on mRNA expression of TNFα and RNF213. LPS stimulated Raw 264.7 cells treated with pioglitazone showed significantly reduced expression of TNFα and slightly reduced expression of RNF213. (b) Expression of RNF213 in 3T3-L1 adipocyte cells treated with pioglitazone. Pioglitazone activates PPARγ which in turn reduced the RNF213 expression.

Figure 6 (a) RNF213 expression in 3T3-L1 adipocytes treated with TNFα. Administration of TNFα (1.5 ng/ml) along with the differentiation media causes a constitutive expression of RNF 213 throughout the adipogenesis process up to 12 days (b) PTP1B expression in 3T3-L1 adipocytes treated with TNFα. Similar to RNF213, the expression of PTP1B was high throughout the adipogenesis process up to 8 days.

Figure 7 Immunoprecipitation was performed with fluorescently labeled antibodies for invitro protein expression analysis a) RNF213 and PTP1B expression in 3T3-L1 adipocyte cells at day 2 of differentiation. **b)** RNF213 and PTP1B expression in TNFα treated adipocytes at day 2 of differentiation. **c)** RNF213 and PTP1B expression in adipocytes at day 5 of differentiation. **d)** RNF213 and PTP1B expression in TNFα treated adipocytes at day 5 of differentiation. The expression of RNF213 and PTP1B was increased by TNFα administration and stayed constitutive during the adipogenesis process. **e)** RNF213 and PTP1B expression in a TNFα and TCS401 co-treated adipocytes at day 5 of differentiation. **f)** RNF213 and PTP1B expression in adipocyte cells at day 2 of differentiation treated with only TCS401.The effect of TNFα on the

constitutive expression of RNF213 was nullified when PTP1B was inactivated. RNF213 was indicated in red colour (Alexa488 tagged antibody), PTP1B was indicated in green colour (Cy3 tagged antibody) and the samples were counterstained with DAPI.

Figure 8 (a) Sodium orthovanadate treatment of adipocytes. Sodium orthovanadate at 35 μM reduced the expression of RNF213 at day 2 of differentiation (b) RNF213 expression in TCS401 treated cells. PTP1B specific inhibitor TCS401 abolished the expression of RNF213 as it inactivated PTP1B at 0.29 μM concentration.

Figure 9(a) Oil Red O staining of adipocytes at day 8 of differentiation. . (**i**) Normal adipogenesis process. (**ii**) TNFα treated cells display less number of lipid droplets indicating reduced adipogenesis. **(iii)** TNFα treated cells with TCS401 co-treatment show enhanced number of lipid droplets suggesting the role of PTP1B on adipogenesis. **b**) Gene expression pattern of PPARγ in adipocytes treated with DIM (differentiation induction media), TNFα, and TCS401. PPARγ expression was gradually increasing and it reached the maximum at day 8 in the cells treated with DIM. PPARγ expression was very low in the cells treated with TNFα. This effect was reversed in cells treated with TCS401.

Figure 10 Oil Red O staining was performed on the 8th day for TCS401 treated differentiated adipocytes. Adipogenesis was increased when PTP1B was inactivated. This was confirmed by the increased levels of PPARγ expression as depicted in Figure 8b

Supplementary data 1. List of interacting molecules to predict a molecular interactome dataset of RNF213

Supplementary data 2.List of forward and reverse primers used in the experiment

Supplementary data 3. Co-regulated members of RNF213 cluster

Supplementary data 4. Curated gene expression data of non-diabetic obese PIMA individuals obtained from Gene Expression Omnibus

Figure 1

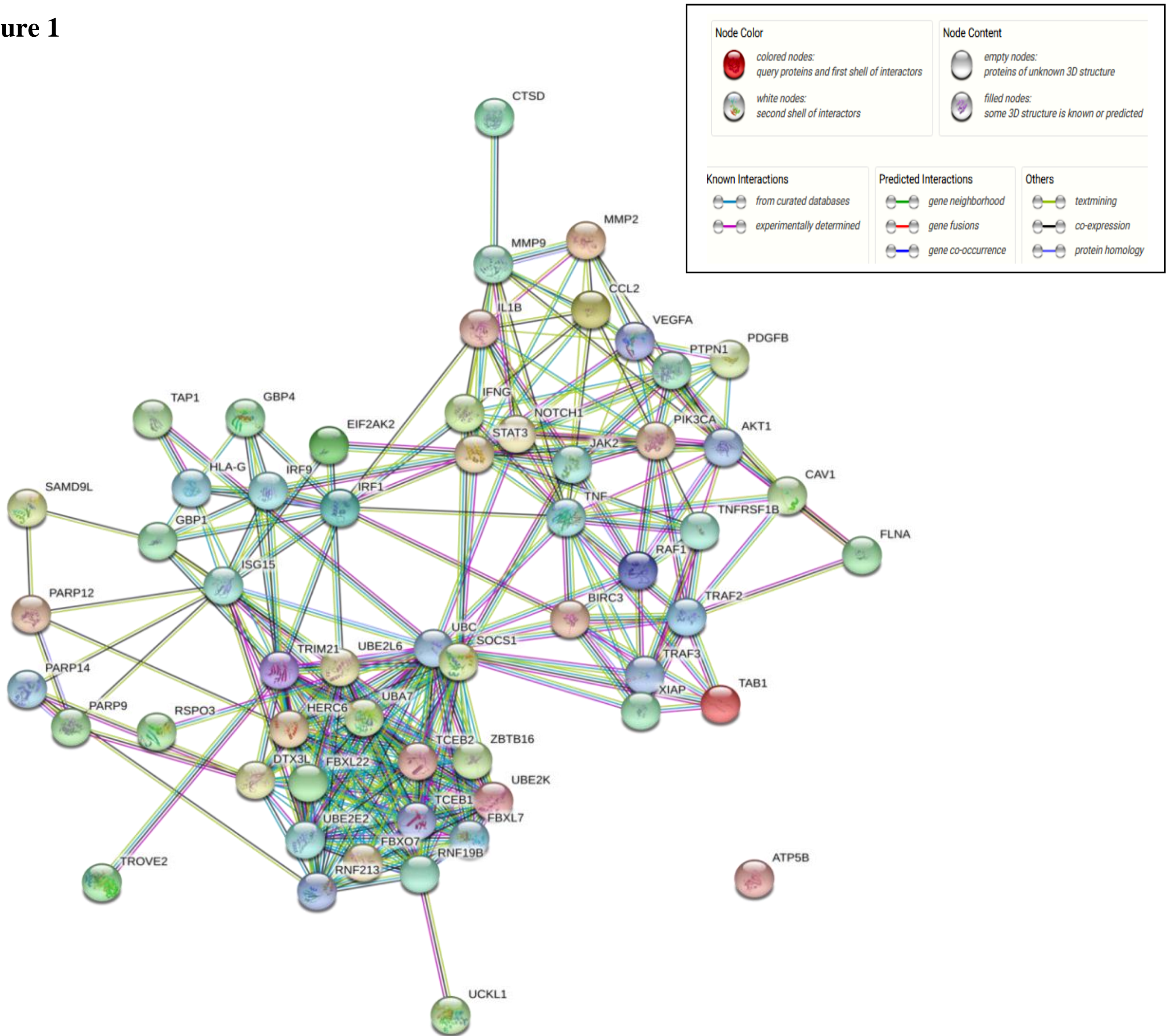

Figure 2

(a)

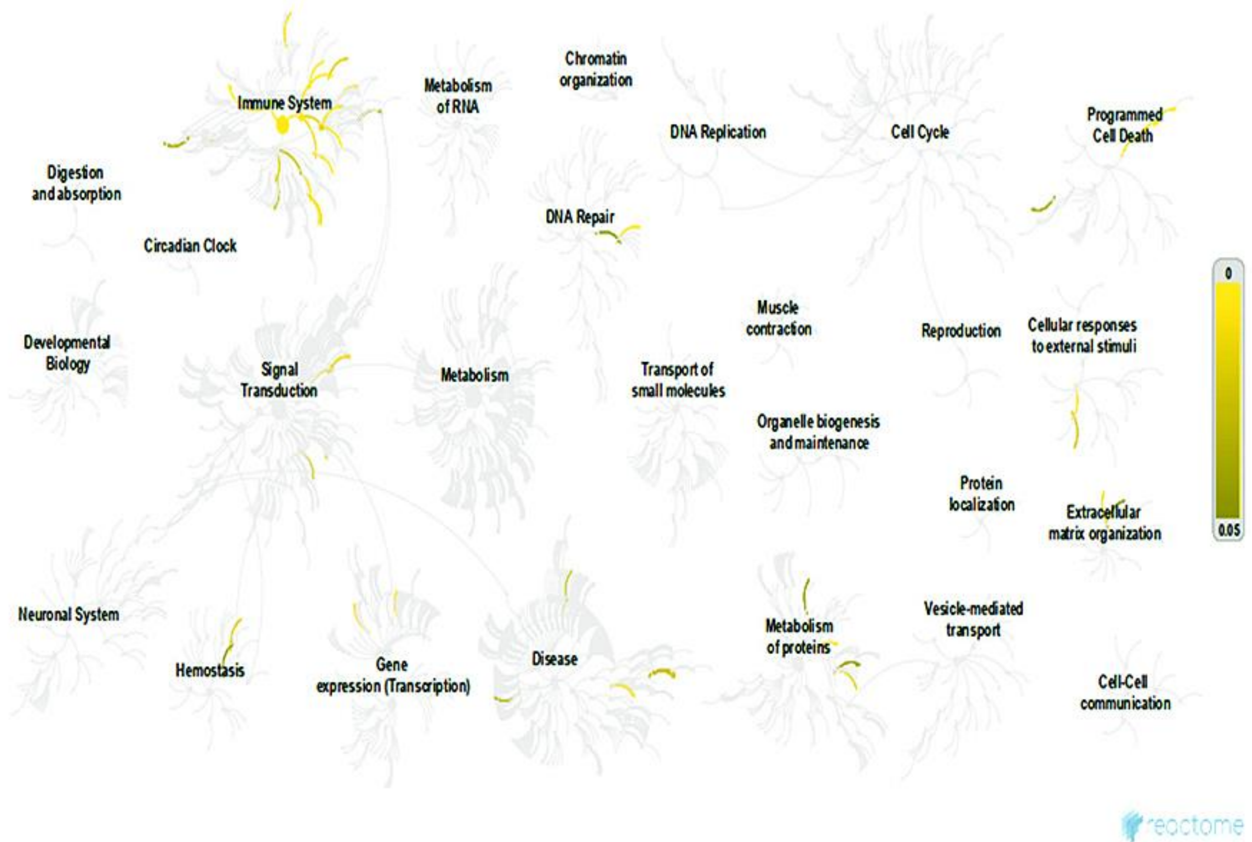

(b)

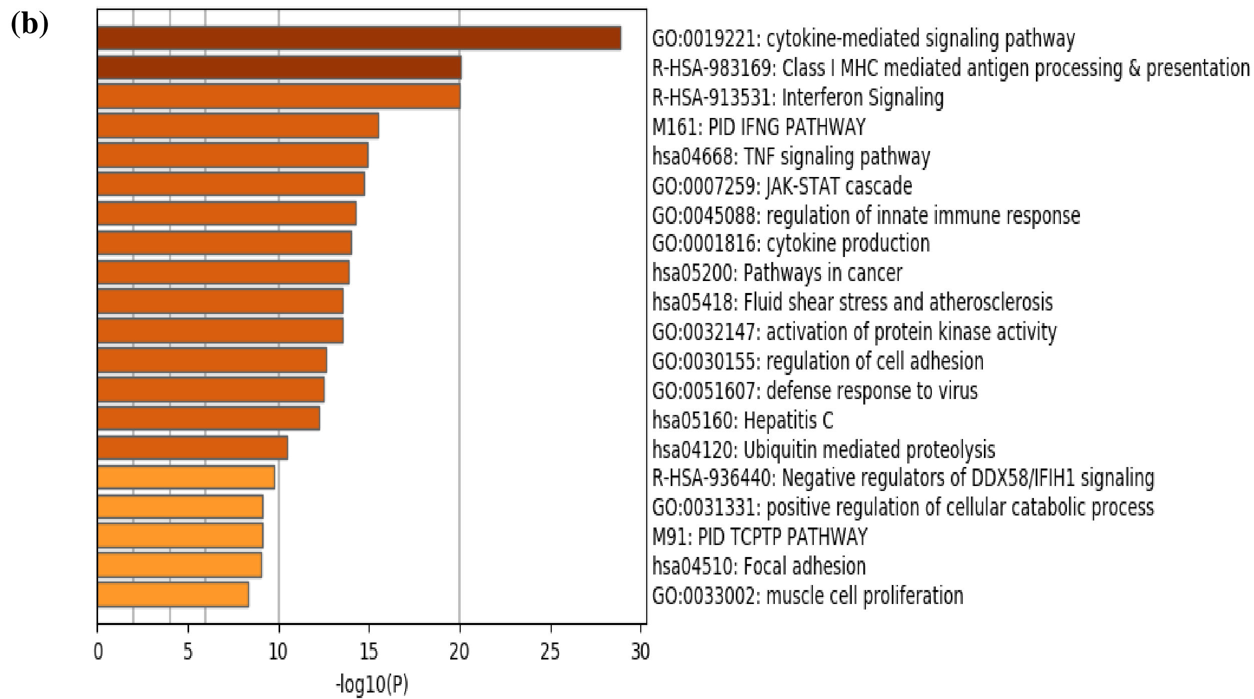

(c)

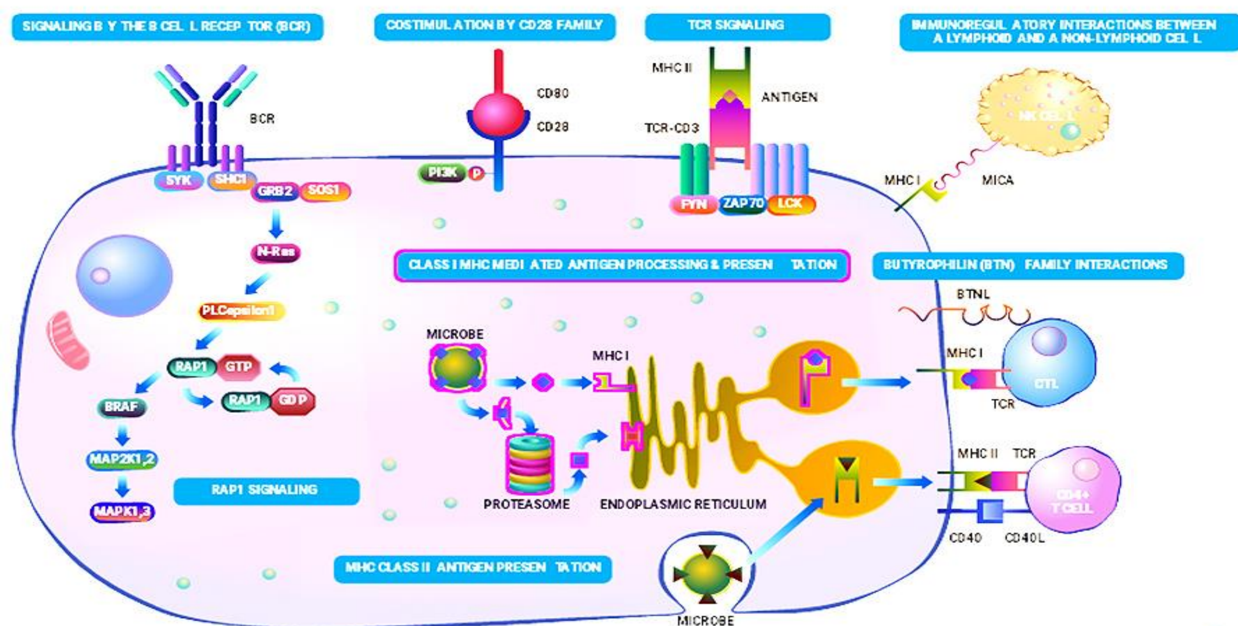

Figure 3

(a)

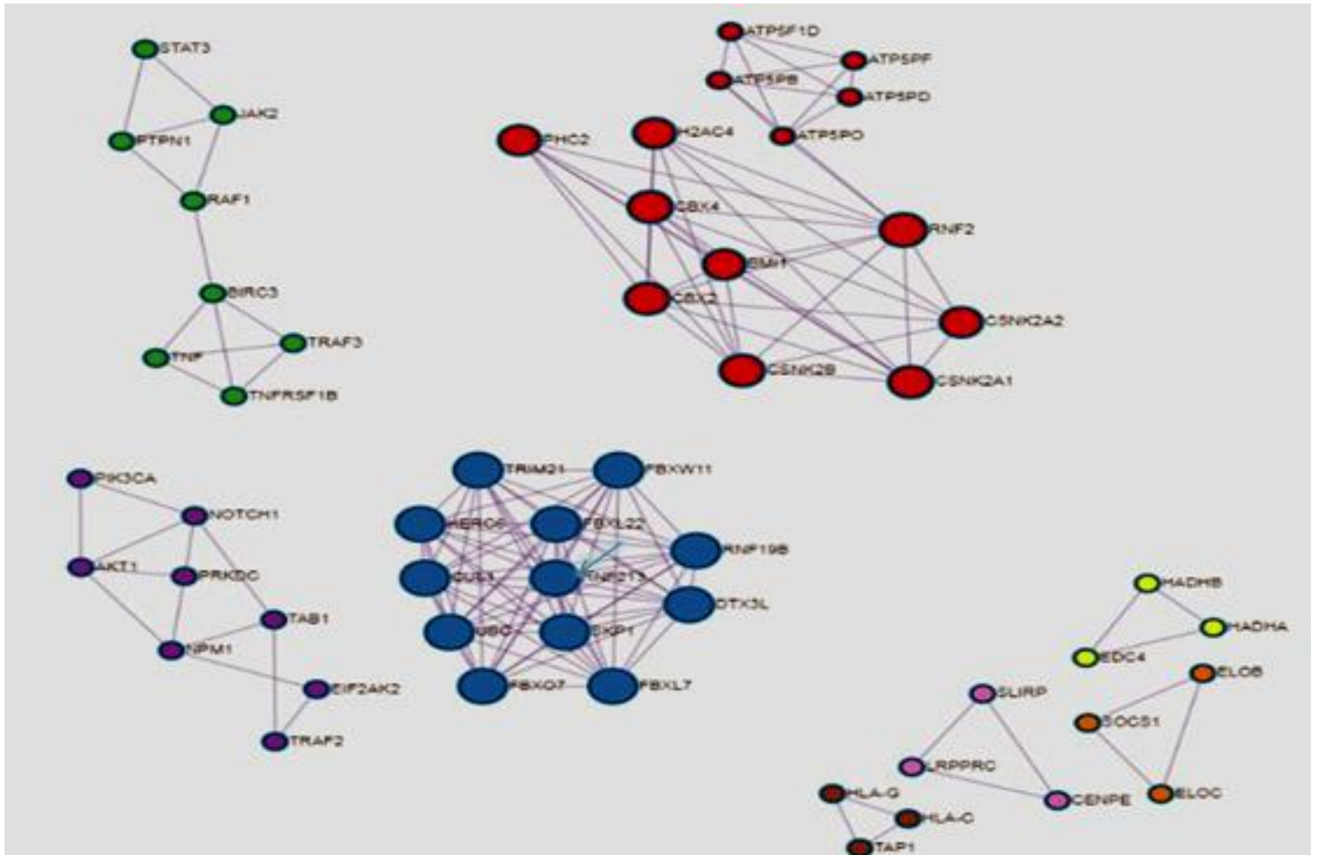

(b)

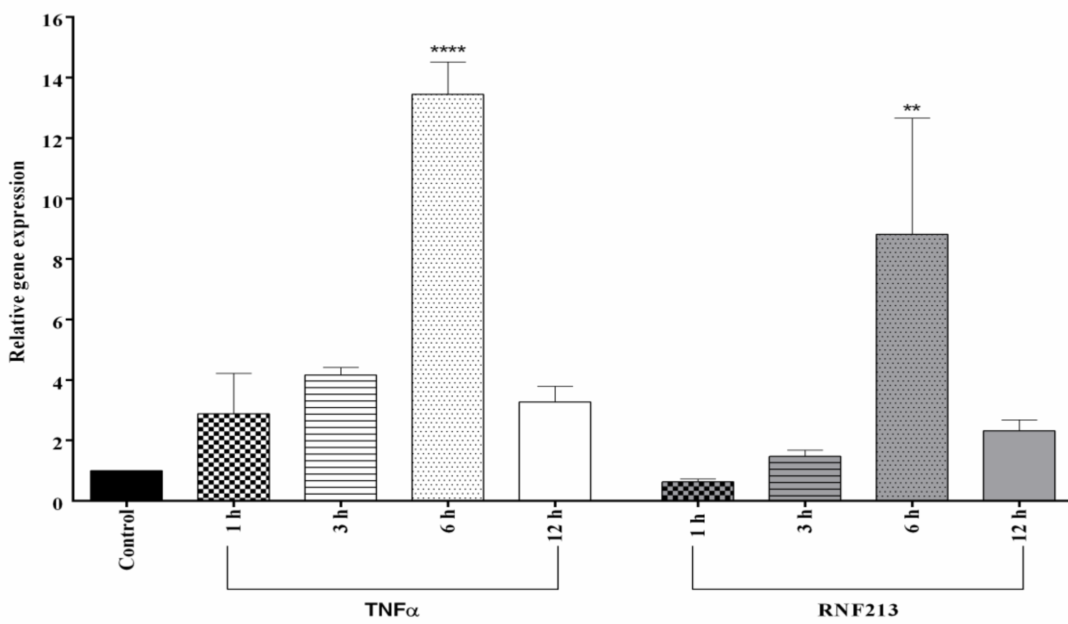

(c)

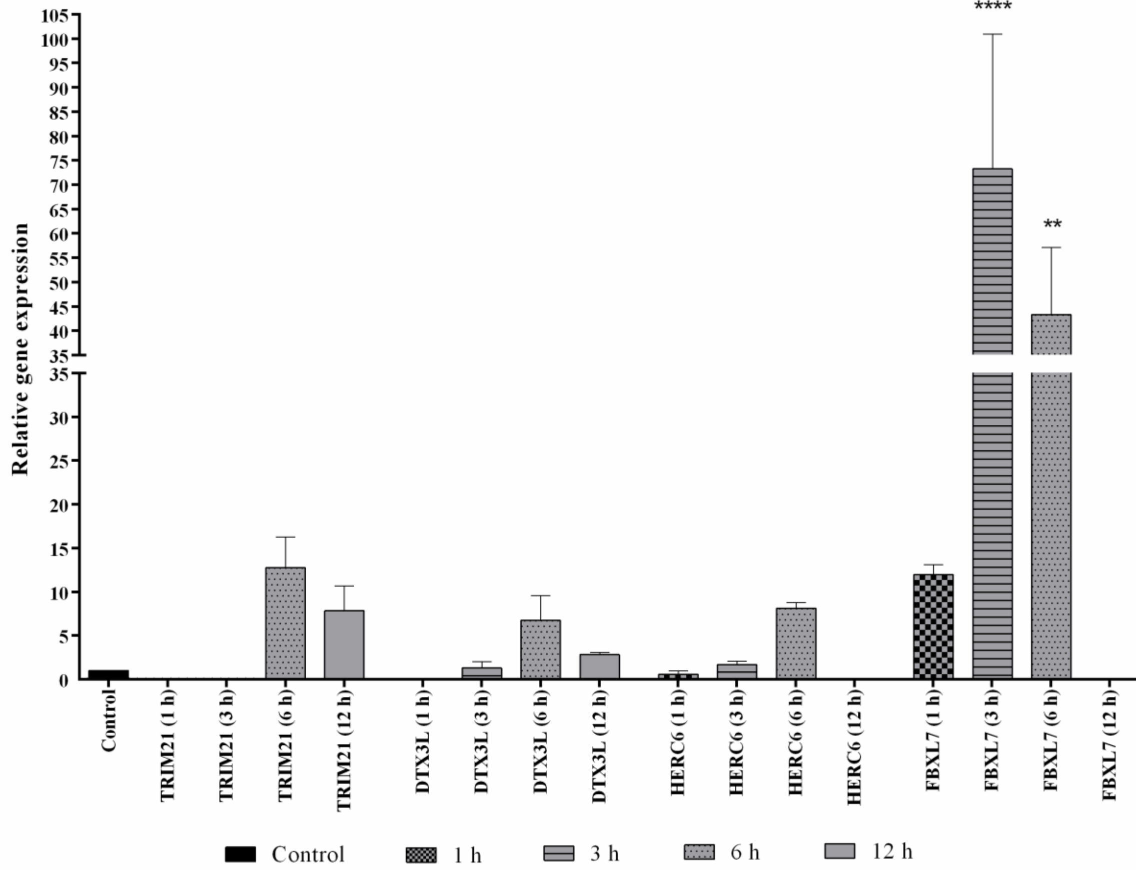

Figure 4

(a)

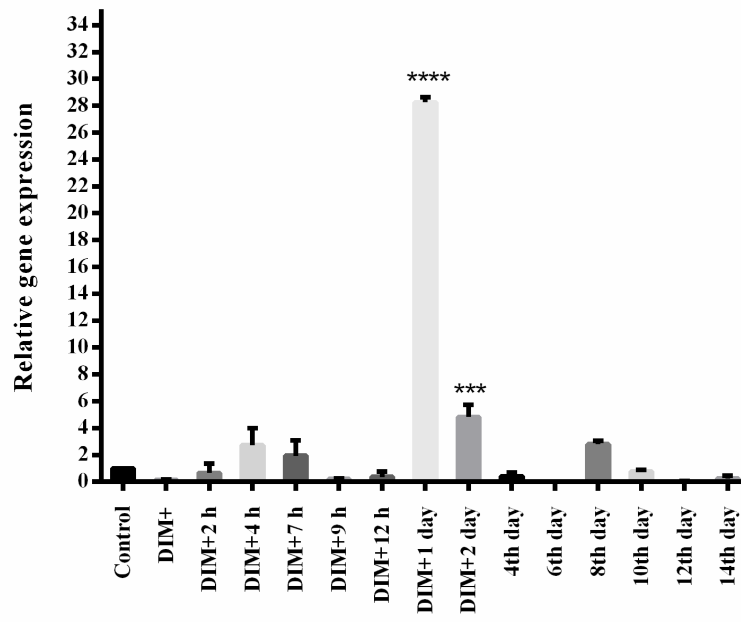

(b)

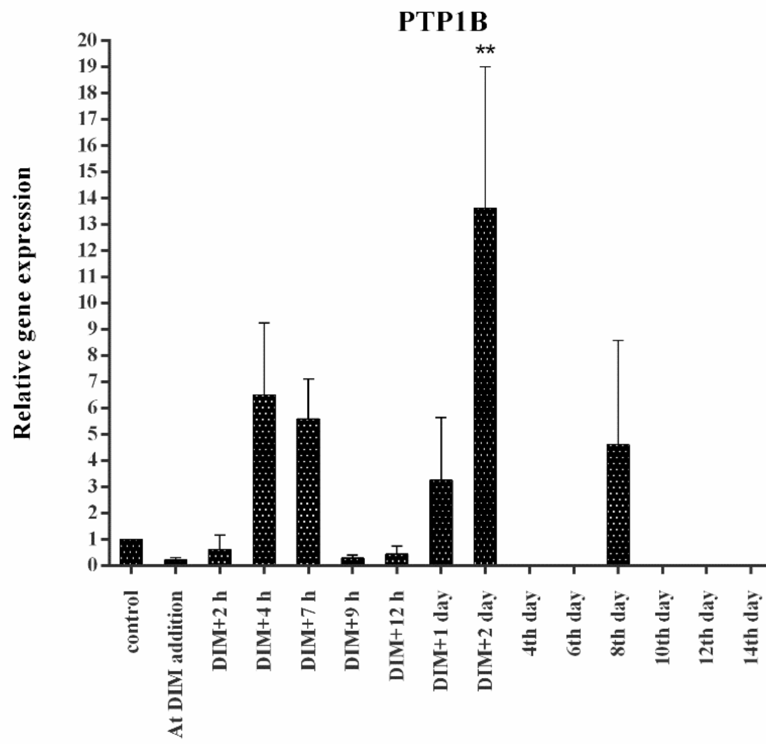

Figure 5

(a)

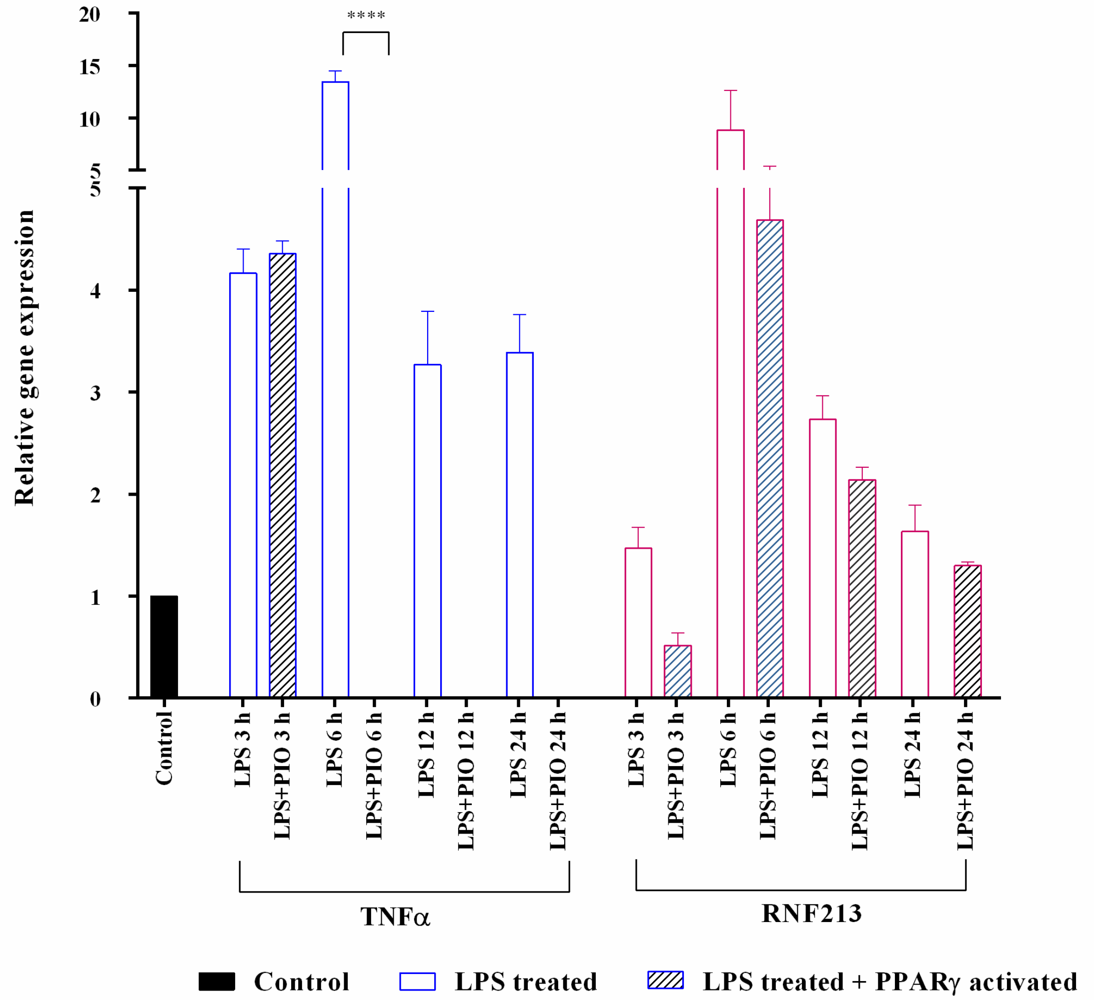

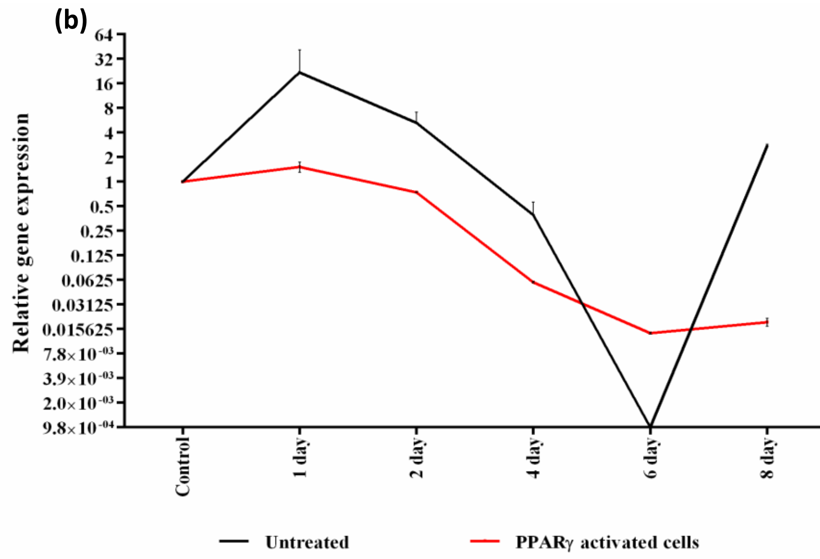
(b)
Relative gene expression
64
32
16
8
4
2
1
0.5
0.25
0.125
0.0625
0.03125
0.015625
7.8×10-03
3.9×10-03
2.0×10-03
9.8×10-04
Control
1 day
2 day
4 day
6 day
8 day
Untreated
PPARγ activated cells

Figure 6

(a)

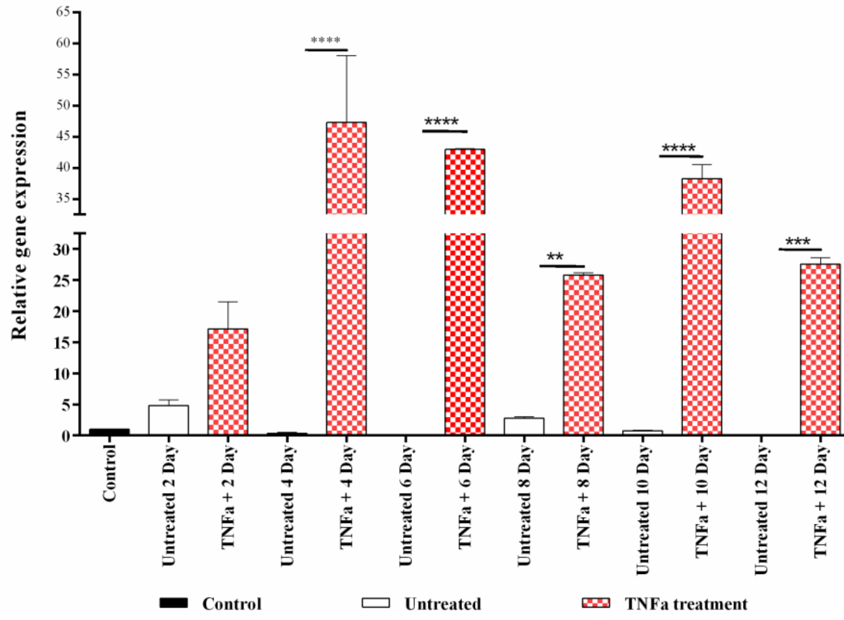

(b)

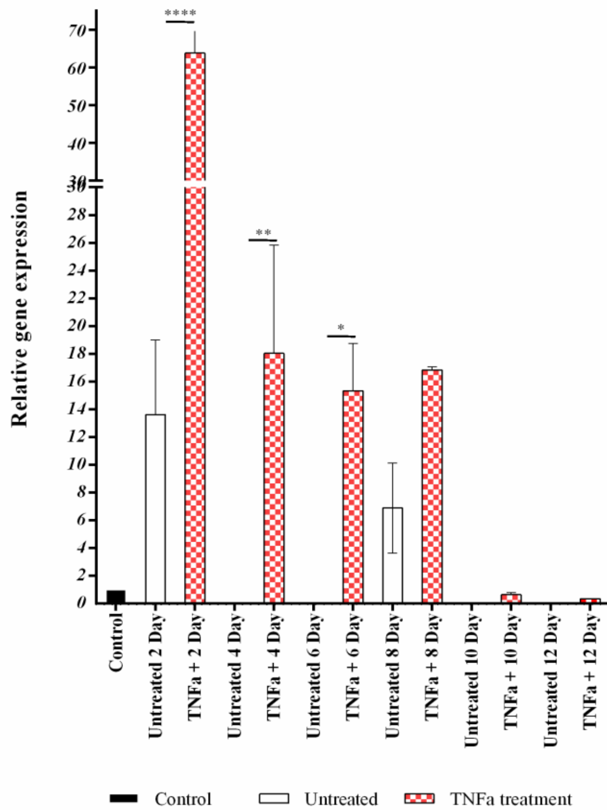

Figure 7

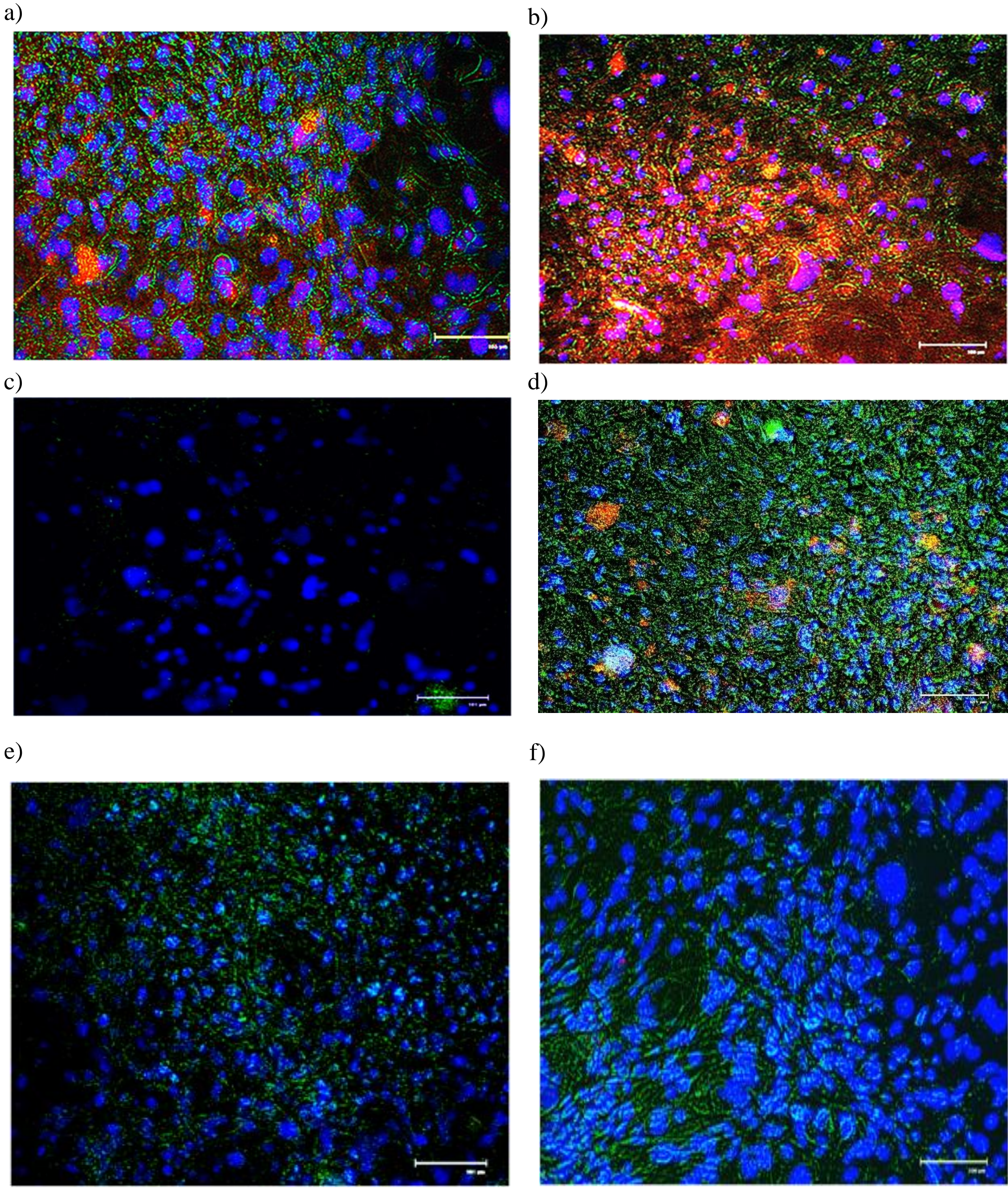

Figure 8

(a)

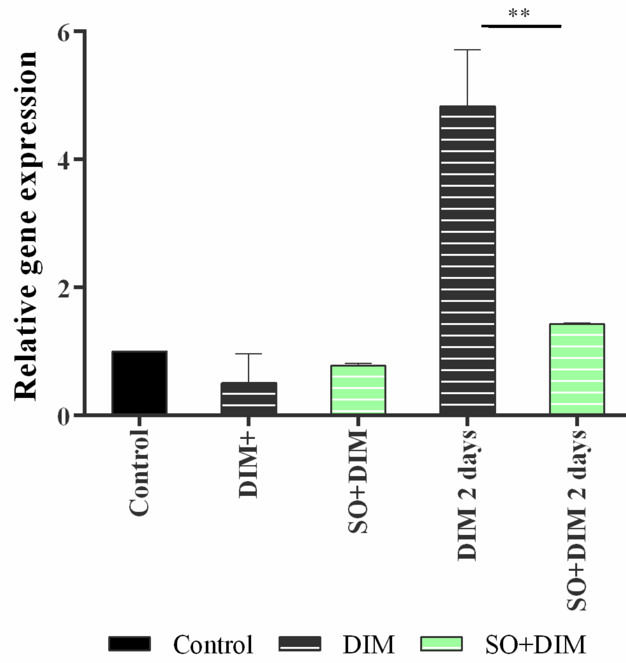

(b)

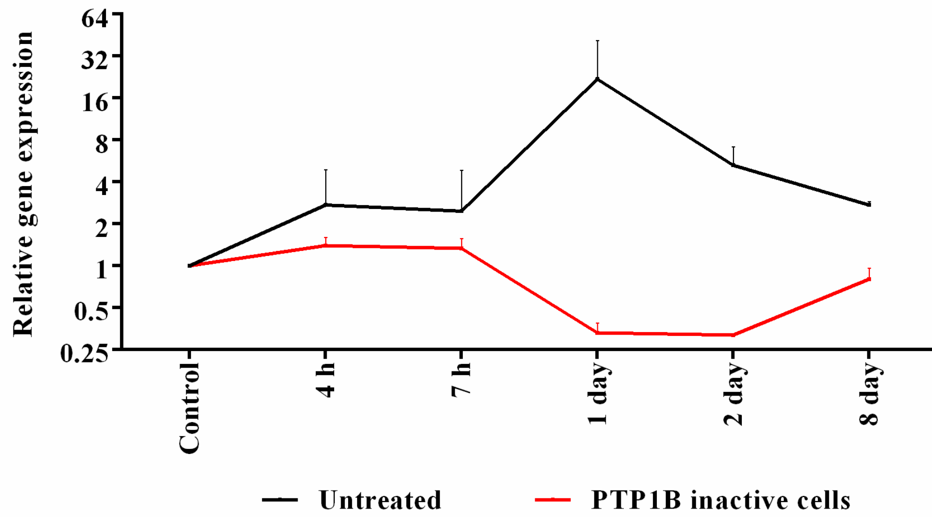

Figure 9

(a)

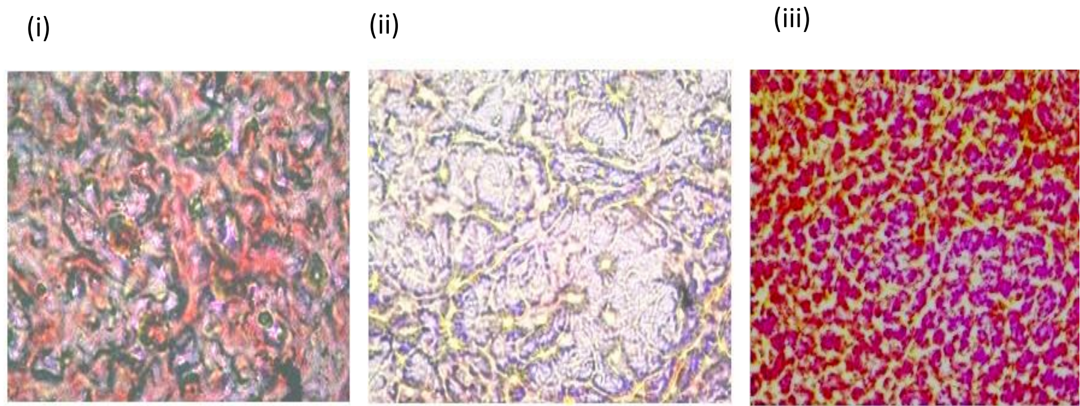

(b)

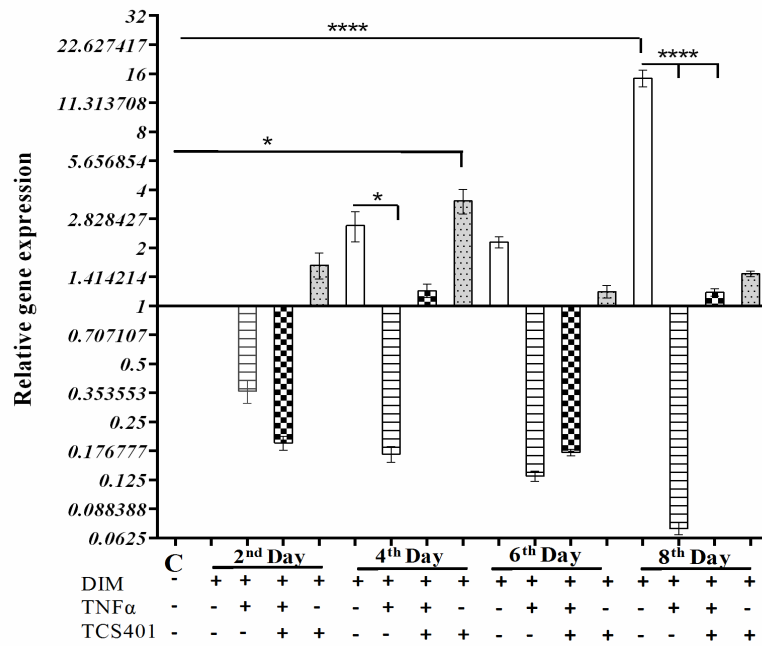

Figure10

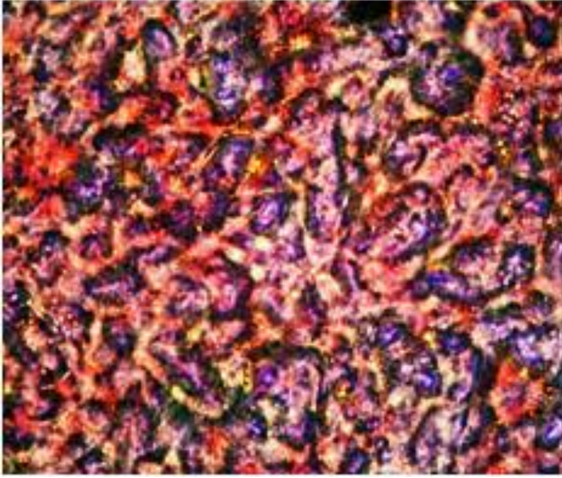

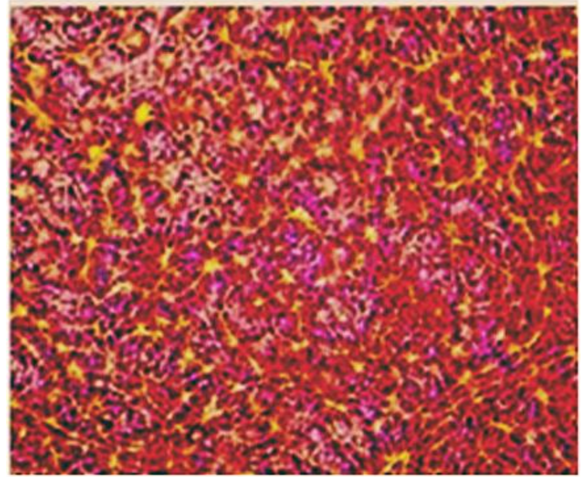

Normal 8th day **TCS401 treated 8th day**

Strategy for interactome prediction